第520回 URSI-F会合資料
開催日：2007年12月14日(金)
場所：情報通信研究機構

POLSAR画像解析を基とした新潟県中越地震の被災住宅の検出

佐藤亮一*　山口芳雄　山田寛喜

新潟大学

Introduction

The Mid Niigata Prefecture Earthquake

- **October 23, 2004　　M6.8**
  - **Large scale landslides at several stricken area**
  - **Unexpected secondary disasters due to the landslides**

Higashi-Takezawa, Yamakoshi (山古志村・東竹沢)

*We express our sincere appreciations to Prof. Makino and NTT data for providing these high resolution photos.

Introduction

Yamakoshi village(山古志村)

Tanesuhara
種苧原

Terano
寺野

POLSAR image analysis

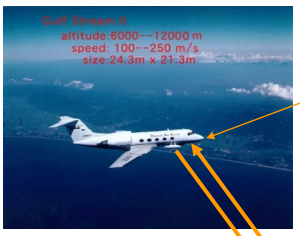

Airborne POLSAR (Pi-SAR**)

Scattered power

Information of polarization

Observation of stricken area in mountainous region

"Yamakoshi village"

**We would like to thank NiCT and JAXA for providing valuable Pi-SAR data sets.

Hybrid classification method

I. Power decomposition

Total power = 

+ 

+ 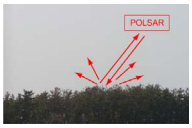

Surface scattering Double-bounce scattering Volume scattering

+ Helix scattering

II. Correlation coefficient

$$\gamma_{XY-AB} = Cor(XY, AB) = \frac{\langle S_{XY} S_{AB}^{*} \rangle}{\sqrt{\langle S_{XY} S_{XY}^{*} \rangle \langle S_{AB} S_{AB}^{*} \rangle}}$$

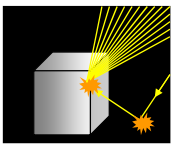

- X,Y,A,B are basis elements - $\langle \cdot \rangle$: ensemble average

Classification method I

Power decomposition

$$\langle [C] \rangle = f_s \cdot [C]_{surface} + f_d \cdot [C]_{double} + f_v \cdot \langle [C] \rangle_{volume} + f_c \cdot \langle [C] \rangle_{helix}$$

Based on “physical mechanism”

Total power = 

+ 

+ 

+ Helix scattering

Surface scattering Double-bounce scattering Volume scattering

$$[C]_{surface} = \begin{bmatrix} |\beta|^2 & 0 & \beta \\ 0 & 0 & 0 \\ \beta^{*} & 0 & 1 \end{bmatrix} \quad [C]_{double} = \begin{bmatrix} 1 & 0 & \alpha^{*} \\ 0 & 0 & 0 \\ \alpha & 0 & |\alpha|^2 \end{bmatrix} \quad \langle [C] \rangle_{volume} = \frac{1}{8} \begin{bmatrix} 3 & 0 & 1 \\ 0 & 2 & 0 \\ 1 & 0 & 3 \end{bmatrix} \quad \langle [C] \rangle_{helix} = \begin{bmatrix} 1 & \pm j\sqrt{2} & -1 \\ \mp j\sqrt{2} & 2 & \pm j\sqrt{2} \\ -1 & \mp j\sqrt{2} & 1 \end{bmatrix}$$

$P(\theta) = 1/2\pi$

Useful marker for man-made targets

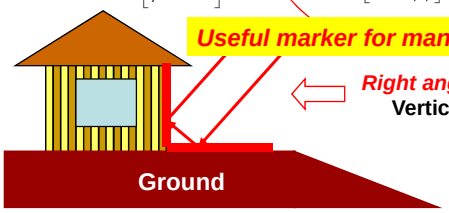

⇐ ***Right angle dihedral structure*:**
Vertical wall and the ground surface.

Classification method I

Power decomposition

Problem of ``Classification method I''

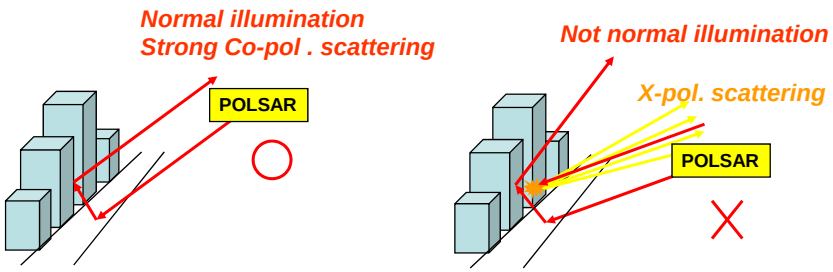

Classification method II

Correlation coefficient

Assumption:

- Residences = Man-made targets
(There exist lots of ``Edges'' on man-made targets)

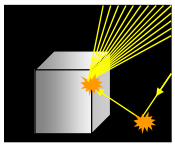

⇩

- "Edge" may be a source generating
"Circular polarized scattering components"

$$[S(LR)] = \frac{1}{2}\begin{bmatrix} a-b+j2c & j(a+b) \\ j(a+b) & b-a+j2c \end{bmatrix} \qquad [S(HV)] = \begin{bmatrix} S_{HH} & S_{HV} \\ S_{VH} & S_{VV} \end{bmatrix} = \begin{bmatrix} a & c \\ c & b \end{bmatrix}$$

$S_{HV} = S_{VH} = c$ for back scattering

⇩

- *Particular polarimetric indices* including *X-component "c"*
for accurate identification of man-made targets.

Classification method II

Correlation coefficient

Polarimetric correlation coefficient

$$\gamma_{XY-AB} = Cor(XY, AB) = \frac{\langle S_{XY} S_{AB}^{*} \rangle}{\sqrt{\langle S_{XY} S_{XY}^{*} \rangle \langle S_{AB} S_{AB}^{*} \rangle}}$$

- X,Y,A,B are basis elements
- $\langle \cdot \rangle$: ensemble average

Co-pol. coefficients for three types of bases

- HV basis (Linear polarization)
- LR basis (Circular polarization)
- XY basis with "45º rotation to HV basis" (Linear polarization)

Classification method II

Correlation coefficient

Co-pol. correlation coefficient for HV basis

$$\gamma_{HH-VV} = Cor(HH, VV) = \frac{\langle S_{HH} S_{VV}^{*} \rangle}{\sqrt{\langle |S_{HH}|^2 \rangle \langle |S_{VV}|^2 \rangle}} = \frac{\langle ab^{*} \rangle}{\sqrt{\langle |a|^2 \rangle \langle |b|^2 \rangle}}$$

No X-polarized component

Unsuitable for man-made target classification?

Scattering matrix for HV basis

$$[S(HV)] = \begin{bmatrix} S_{HH} & S_{HV} \\ S_{VH} & S_{VV} \end{bmatrix} = \begin{bmatrix} a & c \\ c & b \end{bmatrix} \Rightarrow \langle [C] \rangle = \begin{bmatrix} \langle |a|^2 \rangle & \sqrt{2}\langle ac^{*} \rangle & \langle ab^{*} \rangle \\ \sqrt{2}\langle ca^{*} \rangle & \langle 2|c|^2 \rangle & \sqrt{2}\langle cb^{*} \rangle \\ \langle ba^{*} \rangle & \sqrt{2}\langle bc^{*} \rangle & \langle |b|^2 \rangle \end{bmatrix}$$

POLSAR acquires scattering matrix over target region

(S_{HV}=S_{VH}=c for back scattering)

The second order statistics of scattering nature

$\langle \cdot \rangle$: ensemble average

Classification method II

Correlation coefficient

Co-pol. correlation coefficient for LR circular basis

$$\gamma_{LL-RR} = Cor(LL,RR) = \frac{\langle S_{LL} S_{RR}^* \rangle}{\sqrt{\langle |S_{LL}|^2 \rangle \langle |S_{RR}|^2 \rangle}} = \frac{\langle 4|c|^2 - |a-b|^2 \rangle - j4\,\mathrm{Re}\langle c^*(a-b) \rangle}{\sqrt{\langle |a-b+j2c|^2 \rangle \langle |a-b-j2c|^2 \rangle}}$$

Phase

$$\varphi_{LL-RR} = \tan^{-1} \frac{4\,\mathrm{Re}\langle c^*(a-b) \rangle}{\langle |a-b|^2 - 4|c|^2 \rangle}$$

Relationship between RL basis and HV basis

$$[S(LR)] = \begin{bmatrix} S_{LL} & S_{LR} \\ S_{RL} & S_{RR} \end{bmatrix} = \frac{1}{2} \begin{bmatrix} 1 & j \\ j & 1 \end{bmatrix} \begin{bmatrix} a & c \\ c & b \end{bmatrix} \begin{bmatrix} 1 & j \\ j & 1 \end{bmatrix} = \frac{1}{2} \begin{bmatrix} a-b+j2c & j(a+b) \\ j(a+b) & b-a+j2c \end{bmatrix}$$

Classification method II

Correlation coefficient

Co-pol. correlation coefficient for XY basis

(45° rotation)

$$\gamma_{XX-YY} = Cor(XX,YY) = \frac{\langle S_{XX} S_{YY}^* \rangle}{\sqrt{\langle |S_{XX}|^2 \rangle \langle |S_{YY}|^2 \rangle}} = \frac{\langle |a+b|^2 - 4|c|^2 \rangle + j4\,\mathrm{Im}\langle c^*(a+b) \rangle}{\sqrt{\langle |a+b+j2c|^2 \rangle \langle |a+b-j2c|^2 \rangle}}$$

Phase

$$\varphi_{XX-YY} = \tan^{-1} \frac{4\,\mathrm{Im}\langle c^*(a-b) \rangle}{\langle |a-b|^2 - 4|c|^2 \rangle}$$

Relationship between XY basis and HV basis

$$[S(XY)] = \begin{bmatrix} S_{XX} & S_{XY} \\ S_{YX} & S_{YY} \end{bmatrix} = \begin{bmatrix} \cos\theta & \sin\theta \\ -\sin\theta & \cos\theta \end{bmatrix} \begin{bmatrix} a & c \\ c & b \end{bmatrix} \begin{bmatrix} \cos\theta & -\sin\theta \\ \sin\theta & \cos\theta \end{bmatrix} = \frac{1}{2} \begin{bmatrix} a+b+2c & b-a \\ b-a & a+b-2c \end{bmatrix}$$

(θ=45°)

Observation based on POLSAR image analysis

Yamakoshi village

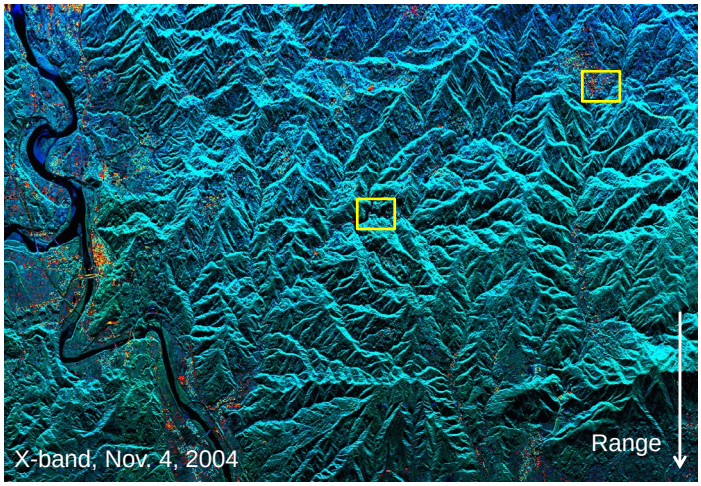

RGB composite (Red: Pd, Green: Pv, Blue: Ps)

Pi-SAR data description

Fully polarimetric data take function

Mode: Quad.Pol. HH+HV+VH+VV

Dual frequency band

	L-band	X-band
Frequency (Wavelength)	1.27GHz (0.236m)	9.55GHz (0.0314m)
Pixel size	2.5m by 2.5m	1.25m by 1.25m
Total pixel number (entire region)	6,000 by 4,000	12,000 by 8,000
Averaging size	5 by 5 pixels	10 by 10 pixels
Incident angle	10/26: 26.91-52.77 [deg.] 11/04: 27.25-53.29 [deg.]	11/04: 27.25-53.29 [deg.]

Measured date

Date: **10/26**/2004 L-band
11/04/2004 L-band **and** X-band

Natural dam detection

Tanesuhara area

Higashi-Takezawa area

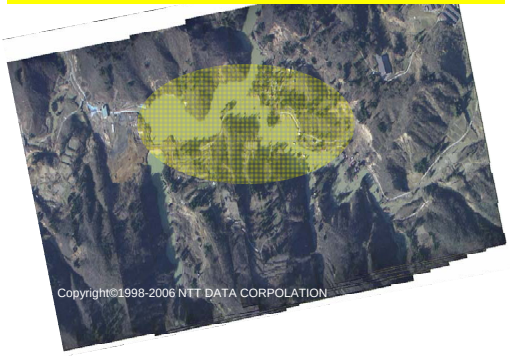

Natural dam detection I

Tanesuhara area

Oct. 26, 2004

L-band

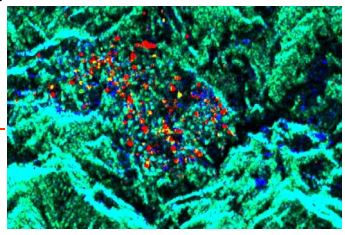

Nov. 4, 2004

L-band

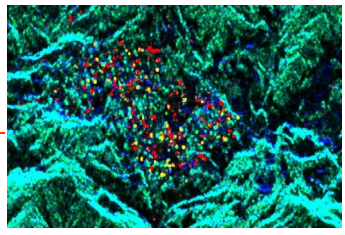

Composite image obtained by ``Power decomposition''

Pd (Double-bounce scattering)

Pv (Volume scattering)

Ps (Surface scattering)

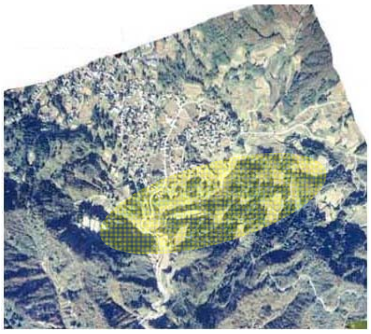

Natural dam detection I

Tanesuhara area

Oct. 26, 2004

L-band

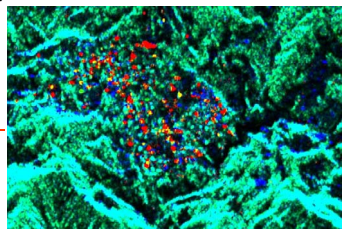

Nov. 4, 2004

X-band

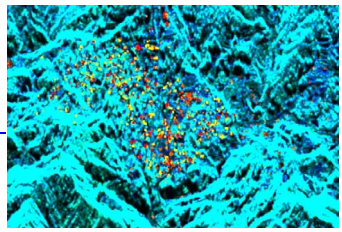

Composite image obtained by ``Power decomposition''

Pd (Double-bounce scattering)

Pv (Volume scattering)

Ps (Surface scattering)

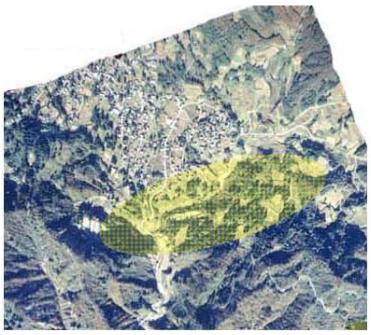

Natural dam detection II

Higashi-Takezawa area

Oct. 26, 2004

L-band

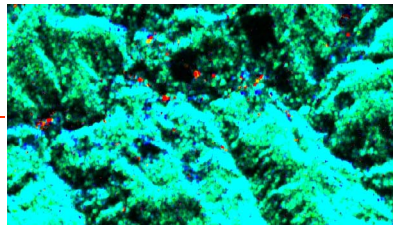

Nov. 4, 2004

L-band

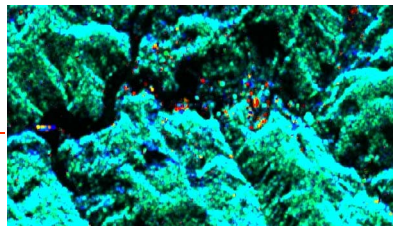

Composite image obtained by ``Power decomposition''

Pd (Double-bounce scattering)

Pv (Volume scattering)

Ps (Surface scattering)

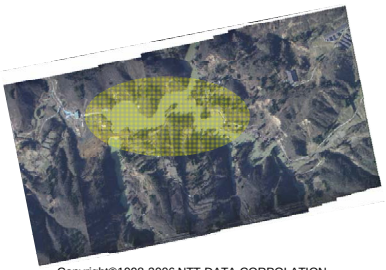

Copyright©1998-2006 NTT DATA CORPOLATION

Natural dam detection II

Higashi-Takezawa area

Oct. 26, 2004

L-band

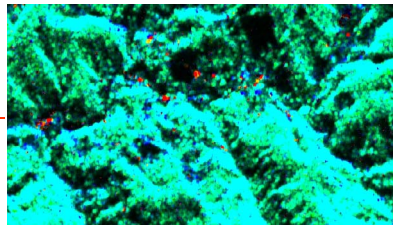

Composite image obtained by ``Power decomposition''

Pd (Double-bounce scattering)

Pv (Volume scattering)

Ps (Surface scattering)

Nov. 4, 2004

X-band

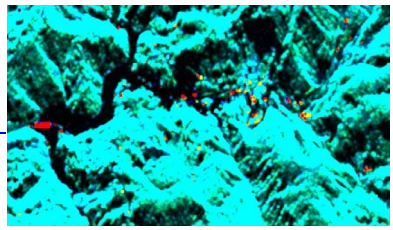

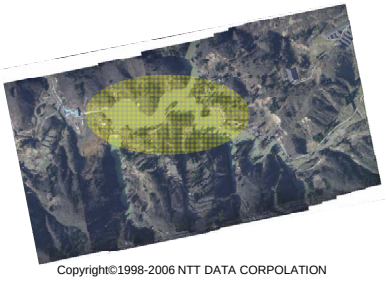

Copyright©1998-2006 NTT DATA CORPOLATION

Man-made target detection I-a

Higashi-Takezawa area

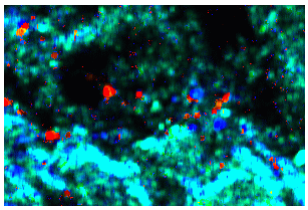

RGB composite image

L-band (1.27GHz)

Oct. 26, 2004
Before flood

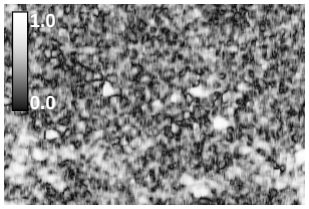

|Cor(HH,VV)|

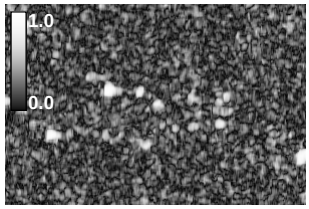

|Cor(LL,RR)|

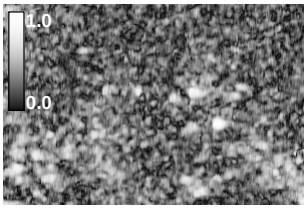

|Cor(XX,YY)|
(45º rotation)

Power decomposition

-- 4 scattering components decomposition --

$$\langle [C] \rangle = f_s \cdot [C]_{surface} + f_d \cdot [C]_{double} + f_v \cdot \langle [C] \rangle_{volume} + f_c \cdot \langle [C] \rangle_{helix}$$

Based on “physical mechanism”

Total power =

+

+

+ **Helix scattering**

Surface scattering | **Double-bounce scattering** | **Volume scattering**

$$[C]_{surface} = f_s \begin{bmatrix} |\beta|^2 & 0 & \beta \\ 0 & 0 & 0 \\ \beta^* & 0 & 1 \end{bmatrix} \quad [C]_{double} = \begin{bmatrix} 1 & 0 & \alpha^* \\ 0 & 0 & 0 \\ \alpha & 0 & |\alpha|^2 \end{bmatrix} \quad \langle [C] \rangle_{volume} = \frac{1}{8} \begin{bmatrix} 3 & 0 & 1 \\ 0 & 2 & 0 \\ 1 & 0 & 3 \end{bmatrix} \quad \langle [C] \rangle_{helix} = \begin{bmatrix} 1 & \pm j\sqrt{2} & -1 \\ \mp j\sqrt{2} & 2 & \pm j\sqrt{2} \\ -1 & \mp j\sqrt{2} & 1 \end{bmatrix}$$

$$P(\theta) = 1/2\pi$$

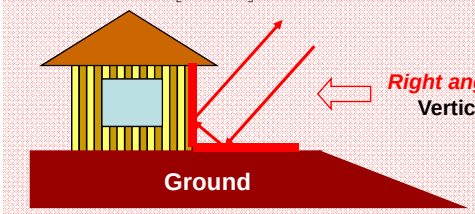

***Right angle dihedral structure*:**
Vertical wall and the ground surface.

Man-made target detection I-b

Higashi-Takezawa area

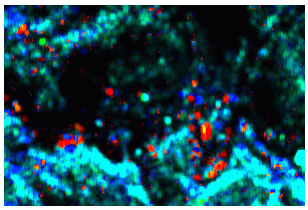

RGB composite image

L-band (1.27GHz)

Nov. 4, 2004
After flood

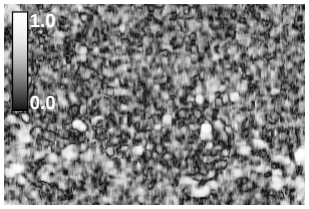

|Cor(HH,VV)|

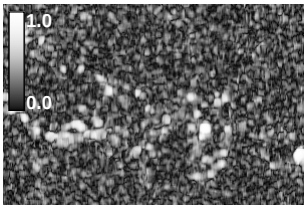

|Cor(LL,RR)|

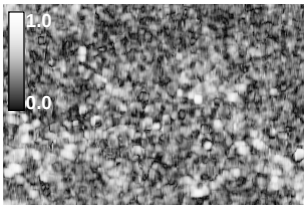

|Cor(XX,YY)|
(45º rotation)

Man-made target detection I-c

Higashi-Takezawa area

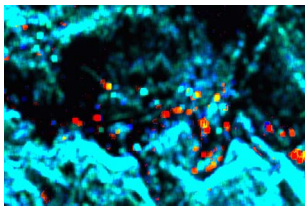

RGB composite image

X-band (9.55GHz)

Nov. 4, 2004
After flood

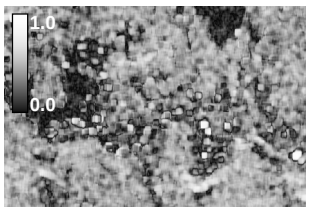

|Cor(HH,VV)|

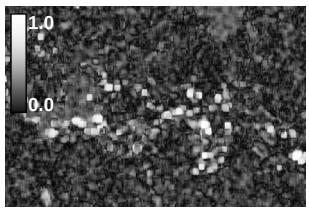

|Cor(LL,RR)|

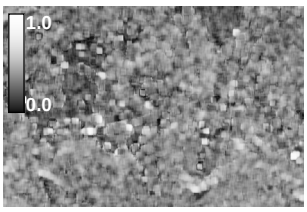

|Cor(XX,YY)|
(45° rotation)

What is back-scattered?

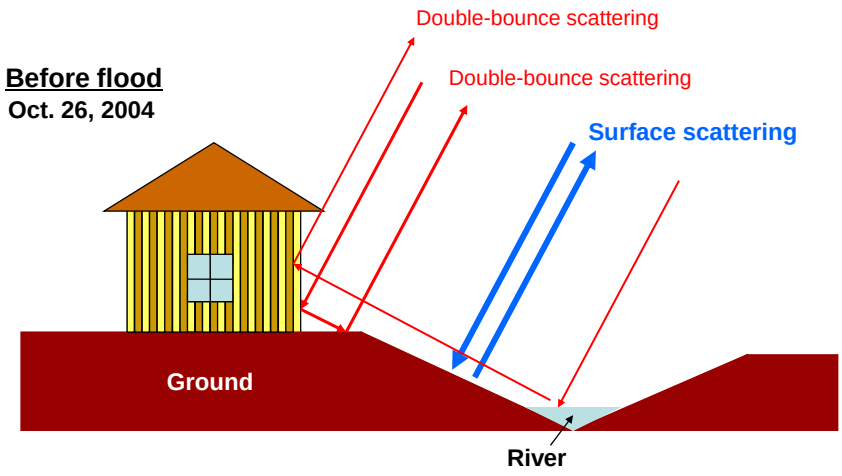

What is back-scattered?

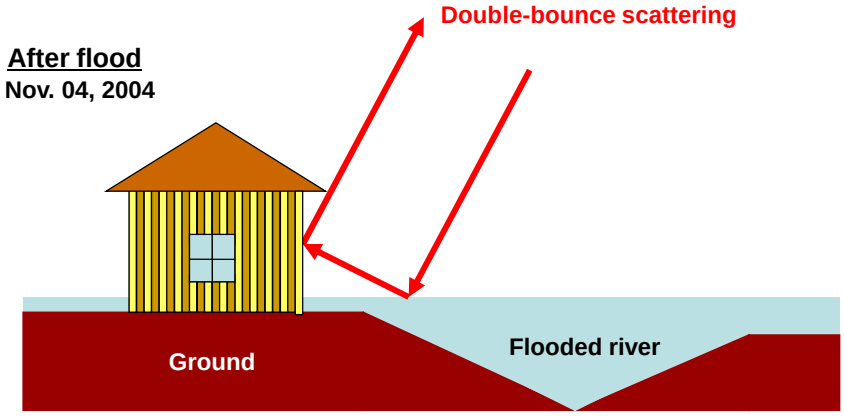

***Double-bounce scattering* is enhanced.**

Reflection symmetry or not?

Reflection symmetry

$$\left\langle S_{HH}S_{HV}^{*}\right\rangle \approx \left\langle S_{VV}S_{HV}^{*}\right\rangle \approx 0 \quad i.e.\ \left\langle ac^{*}\right\rangle \approx \left\langle bc^{*}\right\rangle \approx 0$$

This condition is derived from experimental results.

→ **No residence, Many trees (Forest)**

Co-pol. correlation coefficient for LR basis

$$\gamma_{LL-RR}^{(0)} = Cor^{(0)}(LL,RR) = \frac{\left\langle 4|c|^{2} - |a-b|^{2}\right\rangle}{\left\langle 4|c|^{2} + |a-b|^{2}\right\rangle}$$

Real

Phase

0 or π

Non-reflection symmetry → **Many residences or man-made targets**

Co-pol. correlation coefficient for LR basis

$$\gamma_{LL-RR} = Cor(LL,RR) = \frac{\left\langle 4|c|^{2} - |a-b|^{2}\right\rangle - j4\,\mathrm{Re}\left\langle c^{*}(a-b)\right\rangle}{\sqrt{\left\langle |a-b+j2c|^{2}\right\rangle \left\langle |a-b-j2c|^{2}\right\rangle}}$$

Complex

Phase

$$\varphi_{LL-RR} = \tan^{-1}\frac{4\,\mathrm{Re}\left\langle c^{*}(a-b)\right\rangle}{\left\langle |a-b|^{2} - 4|c|^{2}\right\rangle}$$

Man-made target detection II

Higashi-Takezawa area

L-band image (1.27GHz)

Oct. 26, 2004
Before flood

Nov. 04, 2004
After flood

Pd
Pv
Ps

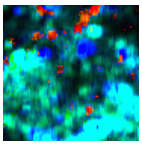
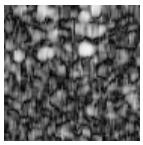

Composite image |Cor(LL,RR)|

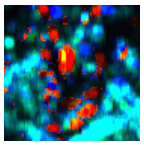
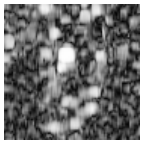

Composite image |Cor(LL,RR)|

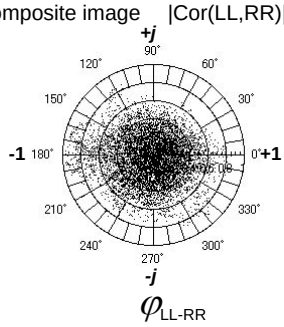

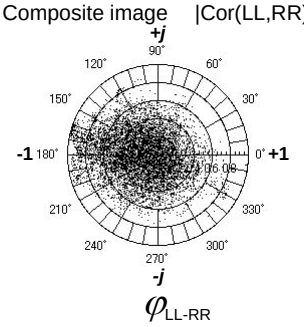

Man-made target detection II

Higashi-Takezawa area

L-band image (1.27GHz)

Nov. 04, 2004
After flood

|Cor(LL,RR)| >0.8
φ_{LL-RR} is not 0 or π

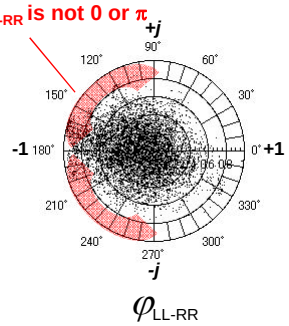

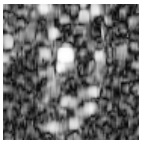

Extract the data under |Cor(LL,RR)|>0.8

White: |Cor(LL,RR)| >0.8
Black: |Cor(LL,RR)| <0.8

Summary of the man-made target classification scheme

Step 1. Power decomposition

- Extract ***double-bounce scattering*** for wide area image

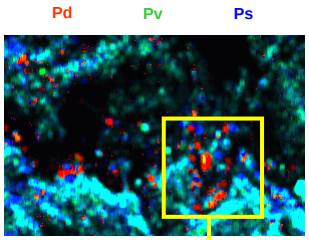

Composite image

Step 2. Further extraction under the conditions as

- **|Cor(LL,RR)|>0.8**
- **$\varphi_{LL\text{-}RR}$ is not 0 or π**

(Correlation coefficient for LR basis)

for the extracted small area image

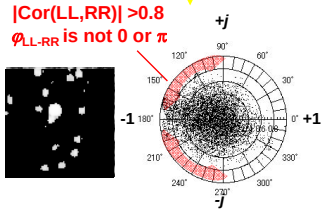

|Cor(LL,RR)| Ang{Cor(LL,RR)}

$\varphi_{LL\text{-}RR}$

Modified correlation coefficient[1][2]

Co-pol. correlation coefficient for LR basis

$$\gamma_{LL-RR} = Cor(LL,RR) = \frac{\left\langle 4|c|^2 - |a-b|^2 \right\rangle - j4\,\mathrm{Re}\left\langle c^*(a-b) \right\rangle}{\sqrt{\left\langle |a-b+j2c|^2 \right\rangle \left\langle |a-b-j2c|^2 \right\rangle}}$$

$$\gamma^{(0)}_{LL-RR} = Cor^{(0)}(LL,RR) = \frac{\left\langle 4|c|^2 - |a-b|^2 \right\rangle}{\left\langle 4|c|^2 + |a-b|^2 \right\rangle}$$

Reflection symmetry

$$\left\langle S_{HH} S^*_{HV} \right\rangle \approx \left\langle S_{VV} S^*_{HV} \right\rangle \approx 0$$

$$\left\langle ac^* \right\rangle \approx \left\langle bc^* \right\rangle \approx 0$$

Modified co-pol. correlation coefficient for LR basis [1],[2]

$$\bar{\gamma}_{LL-RR} = Cor(LL,RR)/Cor^{(0)}(LL,RR) = \frac{\left\langle 4|c|^2 - |a-b|^2 \right\rangle - j4\,\mathrm{Re}\left\langle c^*(a-b) \right\rangle}{\sqrt{\left\langle |a-b+j2c|^2 \right\rangle \left\langle |a-b-j2c|^2 \right\rangle}} \cdot \frac{\left\langle 4|c|^2 + |a-b|^2 \right\rangle}{\left\langle 4|c|^2 - |a-b|^2 \right\rangle}$$

[1] D. Shuler, J.-S. Lee, *et al.*, ``Characteristics of polarimetric SAR scattering in urban and natural areas,'' Proc. of EUSAR 2006, CD-ROM, May 2006.

[2] D. Shuler, J.-S. Lee, *et al.*, ``Polarimetric SAR detection of man-made structures using normalized circular-pol correlation coefficient,'' Proc. of IGARSS 2006, pp.485-488(CD-ROM), Aug. 2006.

Man-made target detection III

Higashi-Takezawa area

L-band image (1.27GHz)

Nov. 04, 2004
After flood

- |Cor(LL,RR)|>0.8
- |Ang{Cor(LL,RR)}|<170 º

YES

Extracted result

Pd
Pv
Ps

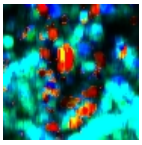

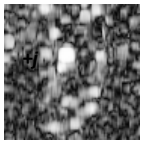

Composite image |Cor(LL,RR)|

Without phase information

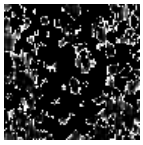

|Cor(LL,RR)|/|Cor$^{(0)}$(LL,RR)|

Man-made target detection III

Higashi-Takezawa area

X-band image (9.55GHz)

Nov. 04, 2004
After flood

- |Cor(LL,RR)|>0.8
- |Ang{Cor(LL,RR)}|<170 º

YES

Extracted result

Pd
Pv
Ps

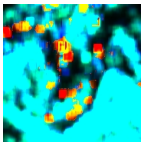

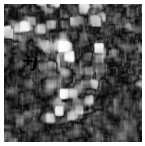

Composite image |Cor(LL,RR)|

Without phase information

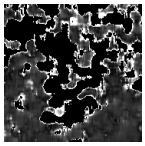

|Cor(LL,RR)|/|Cor$^{(0)}$(LL,RR)|

FDTD polarimetric analysis

Polarimetric scattering analysis for a simple man-made target model by using *the FDTD method*

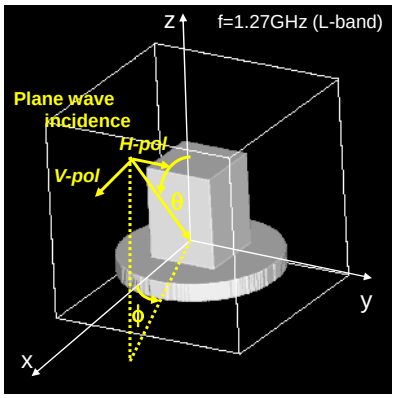

Parameters of the FDTD analysis

Permittivity & conductivity

main part:
ε_r=4 σ=0.0070
(ε_r=4-j0.2 at 1.27GHz)

base part:
ε_r=7 σ=0.0141
(ε_r=7-j0.1 at 1.27GHz)

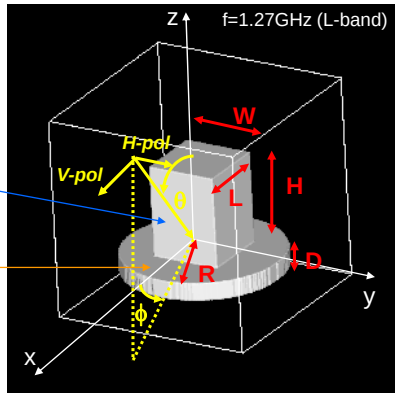

W=L=1.2m (5.08λ)
H=1.6m (6.78λ)
D=0.3m (1.27λ)
R=1.4m (5.93λ)

θ=45 [deg.]
ϕ= 0 to 40 [deg.]

ϕ:variable

Other parameters in FDTD simulation

Analytical region	350 X 350 X 350 cells
Cubic cell size Δ	0.01m
Time step Δt	1.925 X 10^{-11} s
Incident pulse	Lowpass Gaussian pulse
Absorbing boundary condition	Mur 2nd

Statistical evaluation

Evaluation of *statistical* polarimetric scattering feature
as *actual POLSAR image analysis*,

Plain view

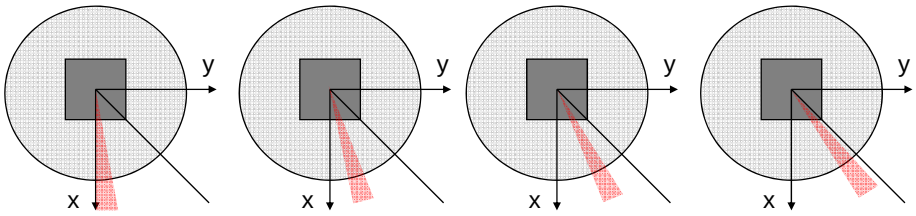

***Ensemble average processing* is carried out for**
***each squint angle range (Average of 10 angles)*.**

Double-bounce squint angular range[3]

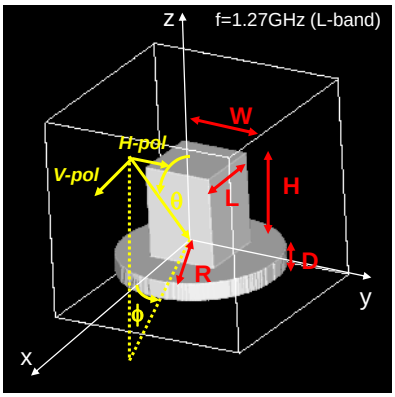

$W = 5.08\lambda,\ \theta = \theta_i = 45^o \qquad X = kW\cos\theta\sin\phi$

$X = \pi \Longrightarrow \phi_c = \sin^{-1}\left(\lambda / 2W\cos\theta\right)$

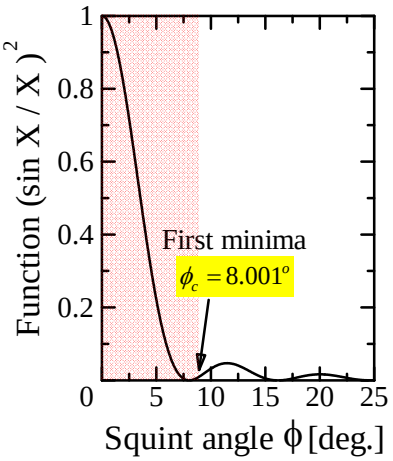

[3] K. Hayashi , R. Sato, Y. Yamaguchi and H. Yamada, ``Polarimetric scattering analysis for a finite dihedral corner reflector,'' IEICE Trans. on Commun., Vol.E89, No.1, Jan. 2006.

Statistical result of the FDTD analysis

Power decomposition

Pt=Pd+Ps+Pv+Pc

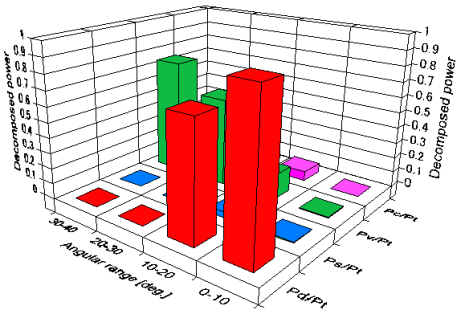

Correlation coefficient (LR basis)

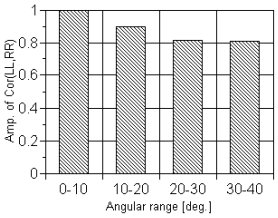

Dielectric model

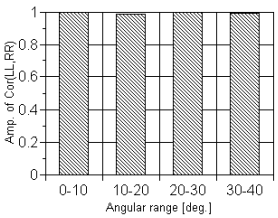

PEC model

Statistical result of the FDTD analysis

Power decomposition

Pt=Pd+Ps+Pv+Pc

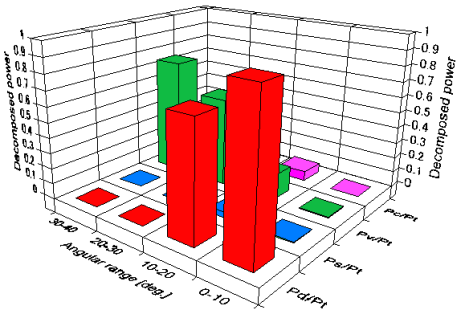

Modified correlation coefficient (LR basis)

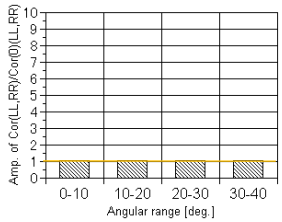

Dielectric model

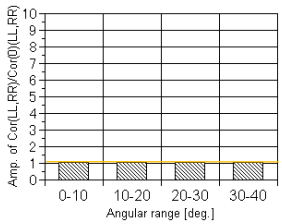

PEC model

Conclusions

Detection of the studded stricken areas
in mountainous region
based on POLSAR image analysis

Hybrid classification procedure

Step 1. Power decomposition

Step 2. Correlation coefficient

⇩

- Achievement of accurate classification of the stricken areas
- Validity has also been confirmed by
  FDTD analysis for simple man-made target model

Acknowledgments

- The authors express their sincere appreciation to NiCT and JAXA, Japan, for providing valuable Pi-SAR image data and to Prof. Makino, Niigata University, and NTT data corp. for providing their high resolution photos around the stricken areas.

- This research was partially supported by a Scientific Research Grant-In-Aid (19510183, 2007) from JSPS (Japan Society for the Promotion of Science), Japan.